JOURNAL OF MATERIALS SCIENCE 13 (1978) 594–610

Cordierite glass-ceramics – effect of TiO_2 and ZrO_2 content on phase sequence during heat treatment

T. I. BARRY, J. M. COX, R. MORRELL
Division of Chemical Standards, National Physical Laboratory, Teddington, Middx., UK

A series of glasses of stoichiometric composition with varying proportions of TiO_2 and/or ZrO_2 as nucleating agent have been studied to examine the effect of nucleation addition on the sequence of crystallization and transformation to the stable phase, cordierite. It is shown that TiO_2 is the most effective nucleating agent and that if large amounts of ZrO_2 are substituted for TiO_2 cristobalite forms as an intermediate phase and is associated with rapid volume changes and consequently with weak porous products. Substitution of ZrO_2 for TiO_2 also causes other changes in phase development, especially in the relative proportions of β-quartz solid solution and magnesian petalite produced during the early stages of crystallization. The use of a combination of experimental techniques (dilatometry, DTA, X-ray diffraction and electron microscopy) has proved most effective in studying phase development and the relationship between processing characteristics and composition.

1. Introduction

A well established method for the production of dense cordierite articles is via the glass–ceramic route [1, 2] in which a monolithic glass body of suitable composition is made to crystallize uniformly throughout its bulk, yielding cordierite as the major phase at the end of the crystallization heat treatment. This method requires that a nucleation agent is added to the original glass to achieve fine-grained crystallization because internal nucleation efficiency is otherwise extremely poor, leading to a predominance of crystal growth from free surfaces. In cordierite compositions, the amount of nucleating agent required depends on type and on the $MgO:Al_2O_3:SiO_2$ ratio of the composition.

There are two stages during the heat treatment of cordierite based glasses where the nucleating agent is of crucial importance. Firstly, efficient nucleation of the β-quartz solid solution metastable phase in a fine-grained state must be accomplished in a reasonable time without excessive deformation of the object, and secondly the microstructure must be controlled in such a manner that the conversion from the β-quartz solid solution to cordierite can be achieved also with a fine-grained structure and without cracking or weakening of the material [3]. The use of 11.5 wt% TiO_2 as nucleating agent has been demonstrated [1, 2] as leading to the successful production of a cordierite ceramic close to stoichiometric composition in MgO, Al_2O_3 and SiO_2. A number of other authors have investigated the nucleation performance of ZrO_2 in silica-rich cordierite glasses [4–8] but not at stoichiometric composition. Of these authors only Zdaniewski [7] has described aspects of the conversion of β-quartz solid solution to cordierite.

In the $Li_2O–Al_2O_3–SiO_2$ system, both TiO_2, ZrO_2, and mixtures of them have been used successfully to make strong spodumene glass–ceramics [9, 10]. The nucleation performance in compositions containing both TiO_2 and ZrO_2 is superior to that containing only either TiO_2 or ZrO_2. This system is rather more easily nucleated that the cordierite system, requiring only 2 to 4 wt% of $TiO_2 + ZrO_2$, whereas glass–ceramics of composition near cordierite generally require at least 10 wt% TiO_2 or ZrO_2 for the production of a

fine-grained ceramic. The primary aim of the work described here was to discover combinations of TiO_2 and ZrO_2 that could give materials of improved performance compared to those containing TiO_2 alone. In the course of the work, the origins of variations of crystallization and transformation were explored, and these form the main subject matter of the paper.

2. Glass–ceramic production and testing

2.1. Raw materials, melting and heat treatment

Since the high temperature mechanical properties of cordierite glass–ceramics are influenced markedly by the raw materials used in making the starting glass [11], due to the segregation of impurities to grain boundaries during crystallization, most of the compositions reported here were made from 'standardized' commercially available raw materials of good quality. Some earlier compositions made from laboratory reagents were also employed in this study, and so Table I lists two batch types A and B for the two sets. The compositions of, or close to, the $MgO:Al_2O_3:2.5\,SiO_2$ stoichiometry of cordierite that were examined are listed in Table II.

TABLE I Raw materials.

Oxide	Grade	Manufacturer
Batch Type A		
SiO_2	Crushed fused quartz	Thermal Syndicate Ltd
Al_2O_3	Analar grade	BDH Ltd
MgO	Analar grade	BDH Ltd
TiO_2	Reagent grade	BDH Ltd
ZrO_2	Reagent grade	BDH Ltd
Batch Type B		
SiO_2	Crushed crystal quartz	Thermal Syndicate Ltd
Al_2O_3	Cera grade	British Aluminium Co Ltd
MgO	Grade III fused	Super Refractories Ltd
TiO_2	Tiona 'VC' grade	Laporte Industries Ltd
ZrO_2	'S' grade	British Aluminium Co Ltd

The raw materials in fine powder form ($\sim 100\,\mu m$) were well mixed on a roller mill, melted in platinum at 1550° C in an electric furnace for 4 h, quenched into water, crushed and remelted at 1550° C. Bars and slabs for test purposes were produced by casting the melt into a heated steel mould previously sprayed with graphite and well polished. When cooled internally to about 750° C, the bars were further cooled in an annealing furnace starting at a temperature about 20° C above the glass transition temperature as determined from a differential thermal analysis (DTA) run. The bars produced were clear and bubble-free, and were a pale to medium brown in colour depending on composition.

Since the composition changes produced large changes in crystallization characteristics, the heat treatment schedule for each composition was determined by the sagging of a small bar using the principle devised by Hagy [12] reported previously [11]. This method indicated the duration and temperature of the nucleation hold required to achieve crystallization without the body sagging unduly. But, as argued earlier [3], it is difficult to maintain such an optimum within a narrow band, even under laboratory conditions, so, in most cases, the hold as determined from deformation was replaced by a slow ramp over the entire temperature range in which sagging was evident. The heating rate during the rest of the cycle was $5°\,C\,min^{-1}$ except during the transformation to cordierite, when it was reduced to about $1.5°\,C\,min^{-1}$ for articles greater than 5 mm thickness to avoid the build up of high stresses owing to gross temperature variations. The general schedule is illustrated in Fig. 1. The maximum temperature was chosen to be that at which transformation was completed within 1 h.

2.2. Property measurements

DTA traces were obtained using a Stanton apparatus with the glass samples melted into platinum capsules to minimize the effects of surface nucleation. Length changes produced during heat treatment were monitored in a Linseis dilatometer, the temperature programme of which was controlled by a Bryans $X-Y$ recorder with a 'line follower' attachment. Thermal expansion coefficients were measured with the same apparatus.

X-ray powder diffraction photographs were produced in a 11.4 cm Debye–Scherrer camera using Cu$K\alpha$ radiation. Phase identification was achieved by comparison with standard specimen films taken on the same apparatus. The maximum error in calculation of unit cell dimensions was about ±0.01 Å, except when the proportion of the phase had fallen to below about 10%. Density measurements were made by water immersion on

TABLE II Glass compositions and properties of fully fired ceramics.

Glass Number	Raw materials group	Composition (wt%)					Glass density ($Mg\,m^{-3}$)	Ceramic density ($Mg\,m^{-3}$)	Overall length change % on firing	Mean bend strength ($MN\,m^{-2}$)	Expansion coefficient 25 to 800° C ($10^{-6}\,K^{-1}$)
		SiO_2	Al_2O_3	MgO	TiO_2	ZrO_3					
Based on stoichiometric cordierite											
G392	B	51.36	34.86	13.78	–	–	–	–*	–*	–	–
C157	A	47.56	32.28	12.76	7.41	–	2.685	–*	–*	–	–
G347	B	46.22	31.37	12.41	10.00	–	2.710	2.613	+1.22	208	2.43
G362	B	45.45	30.85	12.20	11.50	–	2.726	2.633	+1.17	208	2.22
G354	B	45.45	30.85	12.20	6.50	5.00	2.763	2.655	+1.34	180	1.98
G339	B	45.45	30.85	12.20	4.00	7.50	2.780	2.663	+1.46	20	–
G398	B	44.94	30.50	12.06	11.50	1.00	2.742	2.648	+1.17	–	2.19
G384	B	44.94	30.50	12.06	10.00	2.50	2.759	2.659	+1.24	196	2.27
G372	B	44.94	30.50	12.06	7.50	5.00	2.774	2.667	+1.32	210	2.15
G371	B	44.68	30.33	11.99	6.50	6.50	2.778	(2.629)*	(+1.99)*	0	(1.07)
Near stoichiometric cordierite (slightly MgO-rich)											
G100	A	45.50	30.50	12.50	11.50	–	2.726	2.633	+1.17	187	2.20
G315	B	45.50	30.50	12.50	11.50	–	2.726	2.633	+1.17	202	2.20
G292	A	45.50	30.50	12.50	9.00	2.50	2.746	2.638	+1.35	199	2.31
G291	A	45.50	30.50	12.50	6.50	5.00	2.763	2.655	+1.34	180	1.98
G313	A	45.50	30.50	12.50	1.90	9.60	2.795	–*	–*	0	–

*Sample cracked or porous after completion of heat treatment

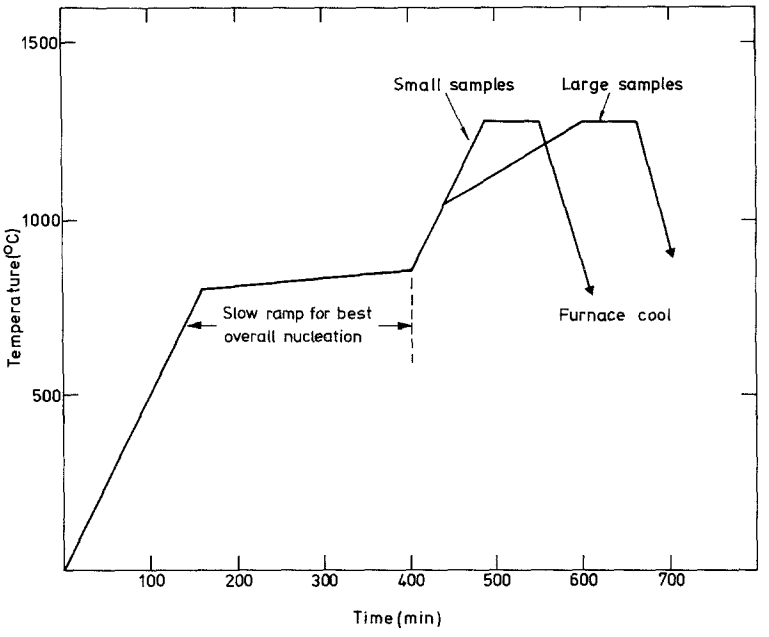

Figure 1 Typical heat treatment schedules.

solid samples since the materials are non-porous except where stated. Specimens of 5 mm x 3 mm section cut from fully heat-treated bars were strength tested in three-point bending over a span of 20 mm.

As discussed previously [3], the total deformation of a glass–ceramic which sags during the initial ceramming can be generalized by the equation

$$\delta = \text{const.} \int_0^{t_c} \frac{dt}{\eta(t, T)}$$

where δ is some measure of the deformation, η is the viscosity, t_c is the time required to crystallize the glass, and the constant term is dependent on load and loading geometry. For the experimental conditions of three-point bending used in the heat treatment sag test, δ was defined as the sag at the centre point, and a parameter D, proportional to δ was calculated. This was a measure of the tendency of a glass composition to deform, but was independent of sample dimensions, i.e:

$$D = \int_0^{T\max} \frac{dT}{\eta(t, T)} = \frac{12\delta ab^3}{Wl^3}$$

where a, b, and l are the width, depth and loading span of the sample, and W is the applied central load. The beam was small enough for its own weight to be negligible compared to W.

The parameter D has the dimensions m^2N^{-1}, can be measured during the heat treatment sag test (Section 2.1.) and allows a comparison of sagging tendencies of various compositions at any stage. It is relatively insensitive to $\dot{\delta}$ and hence to the rate of heating, but does increase slowly with increasing $\dot{\delta}$.

3. Results

For simple reference to nucleation agent content, the following system of abbreviation is used throughout the results and discussion of this work. The glass number, for example G339, is followed by a bracketed term which represents the weight percentages of TiO_2 and ZrO_2, for example (4.0t/7.5z).

To avoid confusion over the naming of individual phases and because of the importance of solid solutions the Appendix describes the nature and occurrence of phases appearing in the relevant part $MgO–Al_2O_3–SiO_2–TiO_2–ZrO_2$ system, both stably and metastably.

3.1. Glass forming characteristics

The glass forming characteristics of the compositions are relatively poor because the viscosities of the melts at the liquidus are low. To test the possibilities for casting large articles without crystallization in the mould, 50 mm x 50 mm cylinders were cast into graphite moulds with 6 mm walls preheated to 500° C and allowed to cool in the moulds. Of the glasses in Table II, G362 (11.5t), which was orange brown in colour, marginally failed

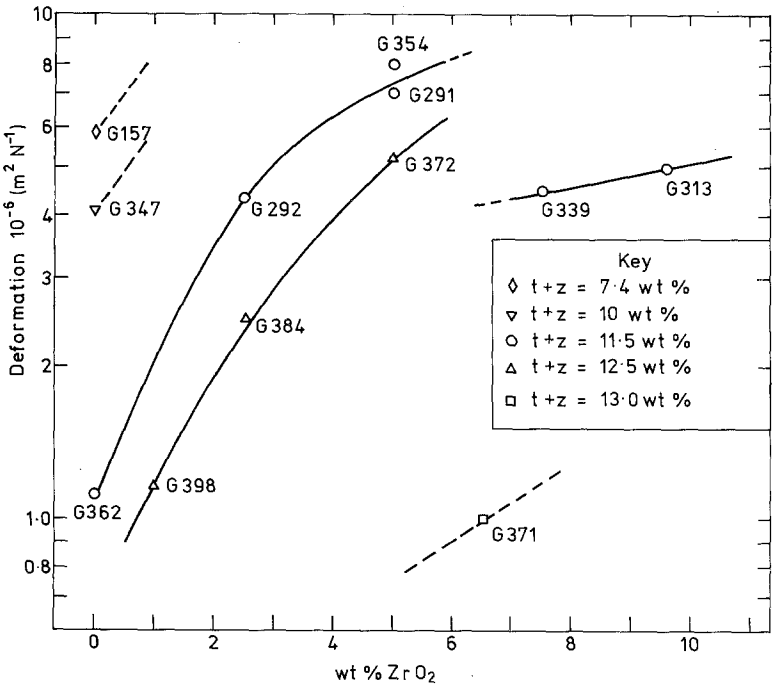

Figure 2 Deformation parameter value as a function of nucleating agent content in stoichiometric cordierite compositions.

this test; small dendrites were found to grow in the centre of the block, whereas G354, in which 5% TiO_2 was replaced by ZrO_2 given a paler coloured glass was free of crystals. On the other hand the addition of only 0.3% Fe_2O_3, or substitution of CeO_2 for TiO_2, caused very pronounced internal crystallization. These results show a marked correlation between the depth of colour in the melt and its tendency to crystallize, presumably because the strongly coloured glasses cooled more slowly internally. The brown colour of the TiO_2 containing glasses was almost certainly caused by colour centres containing both titanium and impurity iron ions since TiO_2 free glasses are not strongly coloured by Fe_2O_3 incorporation and very pure MAS glasses containing TiO_2 are not brown. These facts need to be considered when fabricating thick section articles from cordierite glasses.

3.2. Deformation during initial crystallization

The deformations suffered by the glasses during their conversion to the crystalline state are illustrated in Fig. 2 in terms of the parameter D. The deformation was least for compositions containing most TiO_2. As ZrO_2 replaced TiO_2 on a weight basis the deformation at first increased, but G339 ($4t/7.5z$) and G313 ($1.9t/9.6z$) show relatively low deformations, due to the change in crystal phase initially developed (see Section 3.4.).

3.3. Differential thermal analysis

The principal features shown by the DTA results of Fig. 3 are the glass transition, the initial crystallization, conversion to cordierite and melting. The results are useful for forming an appreciation of trends. However, as the heating rate was 10° C min^{-1} throughout with no hold, the transition temperatures may have been displaced upwards and the transitions themselves may have changed in character compared with standard heat treatments. Fig. 3a shows the traces for the glasses containing no ZrO_2. For G362 ($11.5t$) the glass transition temperature was 760° C, similar to the glasses of lower TiO_2 content in this series. However, the temperature for the onset of crystallization was raised from 885° C for G362 ($11.5t$) to 906° C for G347 ($10t$), to 914° C for G157 ($7.4t$) and to 1050° C when TiO_2 was absent (G392) (presumably surface nucleated in this last case).

Glasses containing high proportions of ZrO_2 gave complex behaviour as illustrated by Fig. 3b. For example, with G339 ($4t/7.5z$) endothermic as well as sharp exothermic effects followed the major crystallization exotherm and preceded melting.

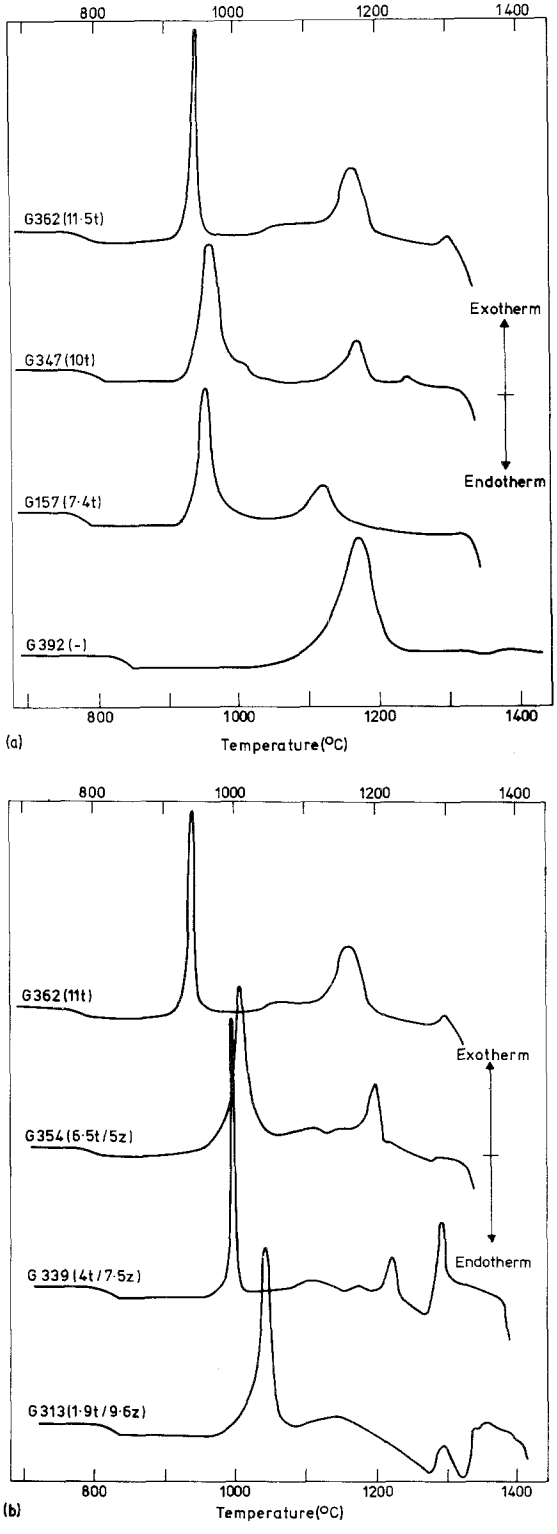

Figure 3 DTA traces of (a) a series of glasses with various levels of TiO_2 (wt%), and (b) a series of glasses with varying levels of TiO_2 and ZrO_2 but with their sum equal to 11.5 wt%.

3.4. X-ray diffraction

For studies of the phase development of these materials, small solid samples were quenched from fixed temperatures during a standard heat treatment. The X-ray analyses are therefore representative of conditions during continuous heat treatment, and cannot be related directly to data in the literature obtained after holds at fixed temperatures, for example to the "time–temperature–transformation" data given by Conrad [6].

A general feature of nucleated cordierite glass–ceramics is the appearance of a β-quartz solid solution phase containing MgO and Al_2O_3 on initial crystallization. On further heating this phase is seen to exsolve MgO and Al_2O_3 and become SiO_2 rich. To monitor the extent of exsolution, standard Debye–Scherrer powder photographs were made of glasses in the series $MgO \cdot Al_2O_3 \cdot nSiO_2$, with n between 2.5 and 10, that had been crystallized to produce β-quartz solid solutions of known compositions. An analysis of unit cell dimensions showed fair agreement with the data of Schreyer and Schairer [13] (Fig. 4). At higher temperatures these compositions did not show an exsolution phenomenon, but tranformed directly to the stable phases cordierite and cristobalite. The extent of exsolution in nucleated materials was then determined from the unit cells calculated to give the best numerical fit with all diffraction lines clearly identifiable with β or α-quartz.

Fig. 5 shows the results for G339 ($4t/7.5z$). For example, the sample heated to 1000° C had a β-quartz cell of $a = 5.24$ Å, $c = 5.31$ Å. These values correspond on Schreyer and Schairer's data to 49 and 37 wt% SiO_2 in the solid solution respectively, with the surprisingly low weighted mean of 45%, a composition with slightly fewer Si than Al atoms. When compared with the data of Fig. 4 from the present work, both a and c correspond to a silica content of 39 wt%, an even lower value. As shown by the work of Schulz *et al* [14, 15], described in the Appendix, unique unit cell values for a given solid solution cannot be expected because of order/disorder effects. Nevertheless, despite some uncertainty in the compositions of the solid solutions calculated in this way, the data can be used to give useful information on exsolution and phase distribution, especially their dependence on temperature, because, as can be seen from Fig. 5, the change of SiO_2 content with

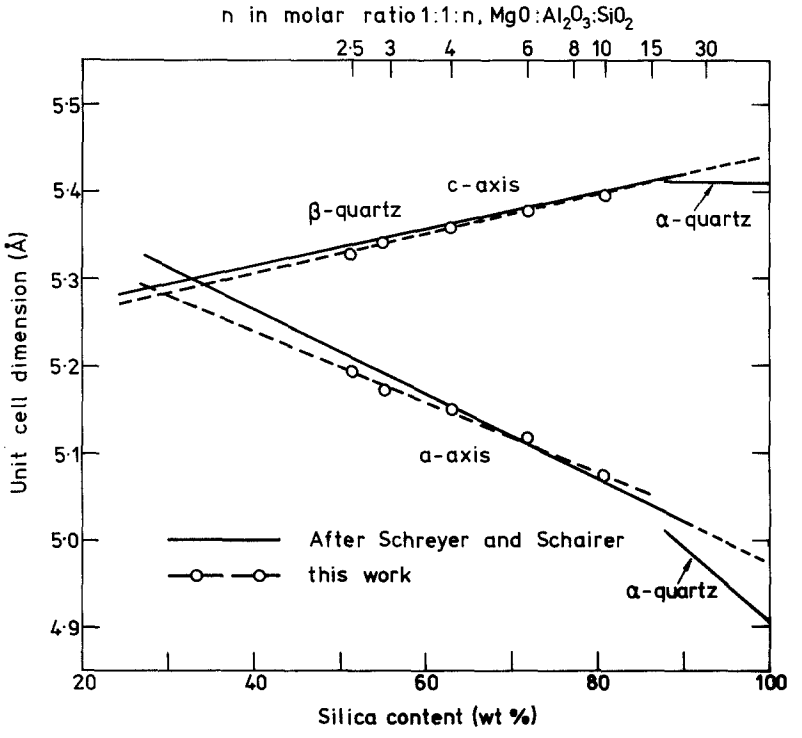

Figure 4 Unit cell dimensions of β-quartz solid solutions obtained in this work from unnucleated glasses of composition MgO: Al_2O_3 :$nSiO_2$ with n varying from 2.5 to 10, compared with those of Schreyer and Schairer [13].

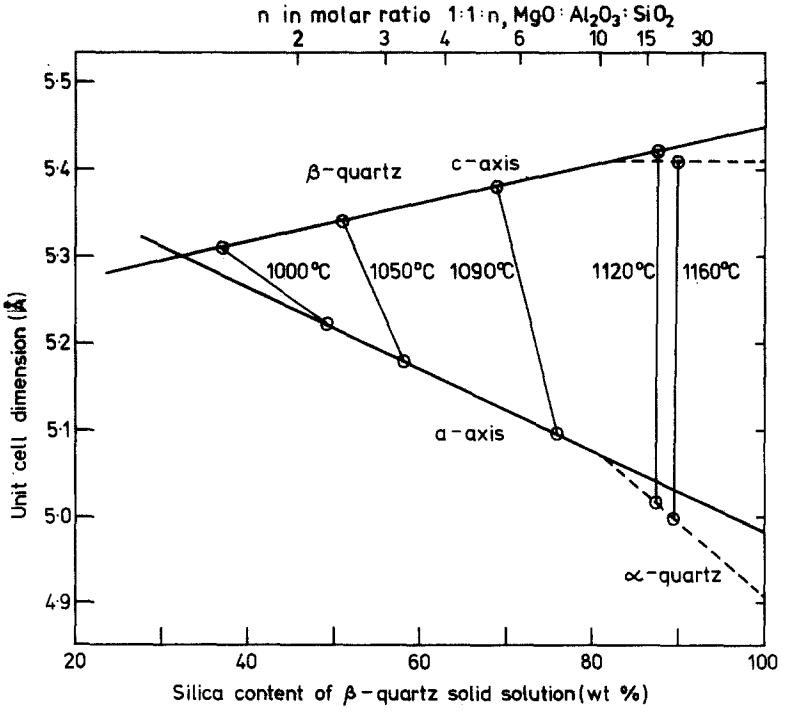

Figure 5 Unit cell dimensions of the exsolving β-quartz solid solution at various temperatures during the heat treatment of G339 ($4t/7.5z$) compared with the data of Schreyer and Schairer [13].

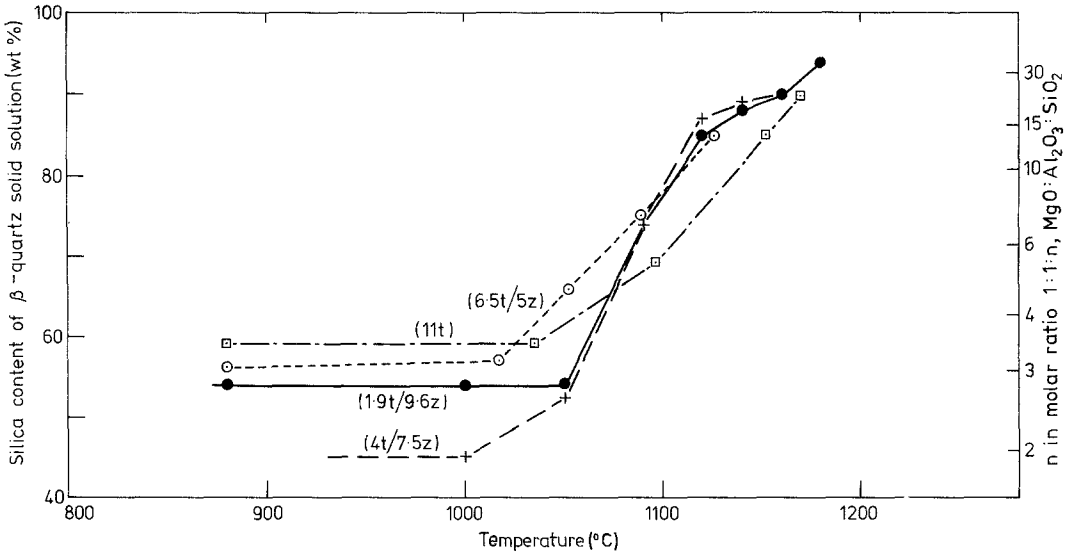

Figure 6 Silica contents of β-quartz solid solutions during heat-treatment at 5° C min^{-1} of glasses in the series TiO_2 + ZrO_2 = 11.5 wt%.

temperature greatly exceeds the uncertainty of measurement.

Fig. 6 shows approximate values of silica content of the β-quartz in the four materials of the series $t + z = 11.5\%$ as determined from a weighted mean using Schreyer and Schairer's data as described above. The results of the four compositions were strikingly different. The very low initial value of 45% SiO_2 for G339 (4*t*/7.5*z*) was less than the 51.4% in the starting glass (neglecting $(t + z)$). On the other hand the value for G362 (11.5*t*) was initially higher than the others but subsequently became the lowest of the four.

Armed with the data so obtained it became possible to estimate the proportion of the various phases produced during the heat treatment of these four compositions. The results shown in Fig. 7 (a to d) were obtained by dividing the components, MgO, Al_2O_3, SiO_2, TiO_2 and ZrO_2, in such a way as to produce proportions of phases that fitted the rough visual assessment of the X-ray diffraction intensities. Each phase was assumed to contain either no MgO and Al_2O_3 or these components in equal proportions. At temperatures over 950° C it was assumed that no glass was present. No amorphous material could be detected by either X-ray or microstructural studies.

In G362 (11.5*t*) the phase development was comparatively simple and has been previously described [3]. The proportion of quartz solid solution decreased at temperatures above 1050° C, at first by the exsolution of spinel and later sapphirine and then from 1150° C onwards by reaction with sapphirine and pseudo-brookite to produce cordierite.

In the composition containing least TiO_2, G313 (1.9*t*/7.6*z*), the phases present at 1000° C were β-quartz solid solution, ZrO_2, magnesian petalite [16, 17], and a little spinel. The β-quartz solid solution has a lower silica content than that produced in G362 (11.5*t*) because the ZrO_2 contains relatively little magnesia and alumina in solid solution compared with pseudo-brookite. However the major difference compared with G362 (11.5*t*) lay in the long persistence of the very silica-rich β-quartz phase and its exsolution product sapphirine between 1100 and 1200° C. When the β-quartz did break down, cristobalite rather than cordierite was the main product. Conversion of cristobalite and sapphirine to cordierite became half-complete only at 1250° C where the reaction suddenly became very rapid. By contrast, the formation of cordierite had reached the same stage in G362 (11.5*t*) at 1190° C and was rather more gradual.

The behaviour of G354 (6.5*t*/5*z*) had many points of resemblance to G362 (11.5*t*); however, there were also differences. The principal phase containing TiO_2 and ZrO_2 was a titania-rich $TiO_2 \cdot ZrO_2$ solid solution that decomposed to give $TiO_2 \cdot ZrO_2$ and rutile at 1150 to 1200° C. The β-quartz solid solution initially contained about

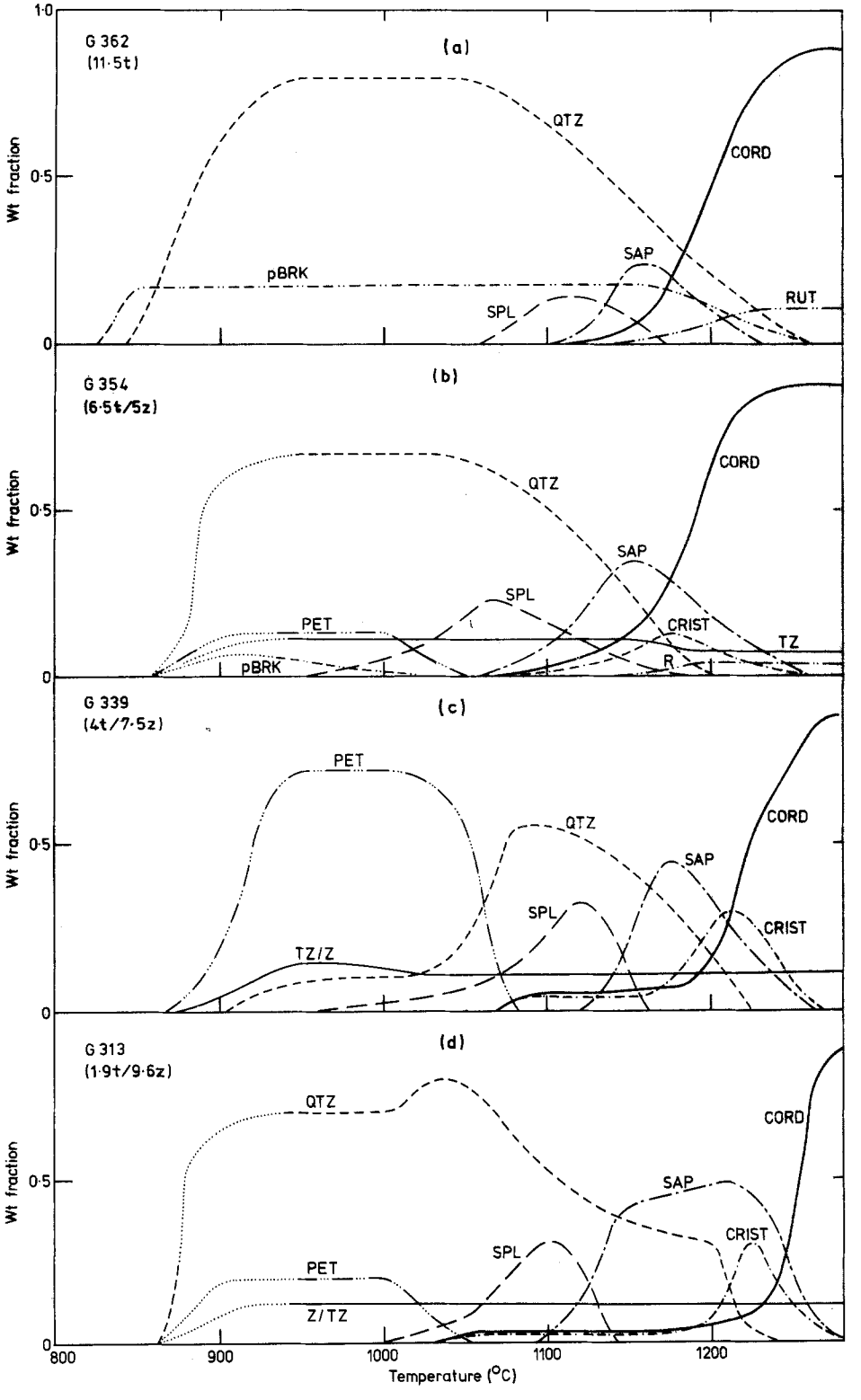

Figure 7 Computed phase content of (a) G362, (b) G354, (c) G339, (d) G313 during heat treatment, based on X-ray data. (Key: QTZ = β-quartz solid solution, pBRK = pseudo-brookite solid solution, TZ = $TiO_2 \cdot ZrO_2$, Z = ZrO_2, PET = magnesian petalite, SPL = spinel, SAP = sapphirine, R = rutile, CRIST = cristobalite, CORD = cordierite).

44% $MgO + Al_2O_3$, but lost this more quickly than the β-quartz in G362 (11.5t). Consequently, although the reaction to form cordierite occurred at a similar temperature, some cristobalite was also formed.

The behaviour of G339 (4t/7.5z) was, in its later stages, intermediate between its neighbours G354 (6.5t/5z) and G313 (1.9t/9.6z), but initially it was strikingly different because a large amount of a magnesian petalite was formed with only a small proportion of β-quartz solid solution. In order to estimate the proportion of petalite it was assigned a $MgO:Al_2O_3:SiO_2$ composition of 1:1:3; for reasons given in the Appendix it seems most unlikely that it can contain less silica than this. The remaining composition was thus rich in magnesia and alumina, and the β-quartz unit cell dimensions confirmed that it had the corresponding composition of about 1:1:2 (46% SiO_2). Because the X-ray pattern of β-quartz was initially faint it seems probable that a significant proportion of the MgO and Al_2O_3 was combined with the TiO_2 and ZrO_2, probably both before and after initial crystallization. A spinel solid solution formed at an early stage in G339 (4t/7.5z). The unit cell was initially 8.036 Å but shifted to 8.060 Å and to the normal value 8.083 Å after the treatments at 1050 and 1090° C. The composition shifts implied by these unit cell variations have a negligible effect on Fig. 7c. Small but significant amounts of cristobalite and cordierite were observed after heat-treatment to 1090° C, when petalite had disappeared, and were probably decomposition products of petalite. The amount of β-quartz, on the other hand, was found to have increased considerably at 1090° C and was probably the major decomposition product.

3.5. Dilatometric length changes

Because of the large deformations associated with the relative difficulty of nucleating the zirconia-containing compositions, the viscous contraction under the load of the contacting rod in the dilatometer caused problems in monitoring true length changes during crystallization at normal heat treatment rates. To avoid this problem, dilatometric runs were performed on samples previously heated to at least 1050° C so that viscous deformation was absent. Fig. 8 shows the length changes in samples of four compositions in the series $t + z = 11.5$ wt% obtained during heating at 5° C min^{-1} through the transformation range up to

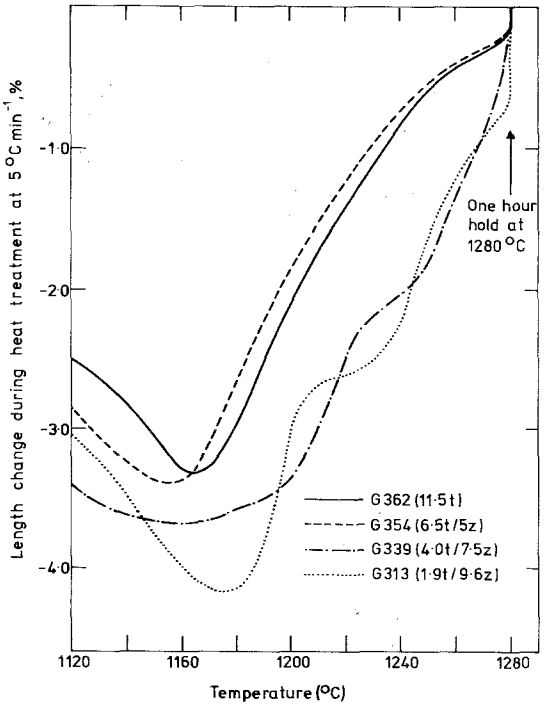

Figure 8 Dilatometric length changes of glasses in the series $TiO_2 + ZrO_2 = 11.5$ wt% during the transformation to cordierite. The length changes are based on the final length after heat treatment at 1280° C for 1 h.

1280° C, followed by a hold of 1 h at that temperature. The results are expressed as % expansion from the reference point of final length at 1280° C, and demonstrate the considerable changes in density that occurred. It is immediately clear that in compositions G339 (4t/7.5z) and G313 (1.9t/9.6z) a higher temperature was required to initiate conversion to cordierite than in G362 (11.5t) and G354 (6.5t/5z), a result which is entirely consistent with Fig. 7.

3.6. Properties of fully heat-treated materials

The strength, density, expansion coefficient and overall glass-to-ceramic change in linear dimensions are recorded in Table II. The mean strengths of all products were in the range 180 to 208 MN m^{-2} for the sample size and surface finish used, except for those products which produced large amounts of cristobalite during heating and were subsequently weak and friable after full conversion to cordierite. The expansion coefficients were all in the range 2.22 to 1.98 × 10^{-6} K^{-1}, the lower values being obtained in materials containing zirconia, or $TiO_2 \cdot ZrO_2$ as a final phase.

In every composition, the starting glass was denser than the final cordierite product. In the absence of viscous deformation during heat treatment there is therefore a net increase in linear dimensions from glass to ceramic of about 1.2 to 1.3%. Compositions which were weak and friable after firing showed rather larger increases, indicating the presence of microcracks and porosity.

4. Discussion

The results presented above show that varying the proportions of TiO_2 and ZrO_2 used to induce fine-grained crystallization had a marked effect on many aspects of the crystallization process and product properties. The aim of this section is primarily to explain the origin of the observed changes and the relationship between them.

4.1. Deformation

The deformation sustained by the specimen before it stiffens due to crystallization is a measure of the difficulty of nucleation and early crystal growth. In lithia–alumina–silica glasses, mixtures of TiO_2 and ZrO_2 give more efficient nucleation than either TiO_2 or ZrO_2 alone [9, 10], whereas in the magnesia–alumina–silica system the deformation is least for TiO_2 alone. The reason for this may be that the pseudo-brookite solid solution that develops when there is a substantial molar excess of TiO_2 over ZrO_2 has a dendritic structure [3] which is much more effective in stiffening the partly crystallized glass than the minute individual particles of ZrO_2 or $TiO_2 \cdot ZrO_2$ solid solution that precipitate when significant amounts of ZrO_2 are also present. The actual crystal size of the β-quartz solid solutions or magnesian petalite that develop is of the order 0.5 to 2.0 μm for all compositions containing 11.5 wt% $TiO_2 + ZrO_2$.

4.2. Occurrence of petalite

Petalite develops to the greatest extent in the composition G339 ($4t/7.5z$). The reason for this is by no means obvious. Holmquist [17] showed that the development of petalite was enhanced in glasses of composition $MgO \cdot Al_2O_3 \cdot n\ SiO_2$ by increasing n. Thus in the present compositions, petalite would be expected to be favoured by the prior or simultaneous formation of a phase that removes some of the MgO and Al_2O_3 from the glass composition. However, although such a phase, pseudo-brookite with the composition $MgO \cdot Al_2O_3 \cdot 3TiO_2$ does develop first in G362 ($11.5t$), no petalite is found in this material despite the fact that the residual glass has a composition close to 1:1:3 compared with the original 1:1:2.5 molar ratio $MgO:Al_2O_3:SiO_2$.

Three tentative explanations can be given for the occurrence of petalite as a major phase in G339 ($4t/7.5z$).

(a) Neilson [4], in his studies of $MgO \cdot Al_2O_3 \cdot 3SiO_2$ with 10% ZrO_2 describes the separation of a ZrO_2-rich amorphous phase prior to crystallization. It is possible that when TiO_2 is also present this amorphous phase is particularly rich in MgO and Al_2O_3, perhaps especially in Al_2O_3, to the extent that the residual glass phase composition is shifted to that favourable for petalite.

(b) It is possible that the phase $TiO_2 \cdot ZrO_2$ provides favoured sites for the nucleation of petalite.

(c) Solid solution of ZrO_2 and/or TiO_2 in petalite or β-quartz may lead to preferences for one or other of these to grow as major phases, dependent on the TiO_2 and ZrO_2 concentrations.

On these suggested explanations, (a) is almost an essential condition for petalite formation, with (b) or (c) as alternative additional stimuli. An examination of the microstructure of G339 ($4t/7.5z$) after heat treatment to 880° C shows only dendritic structures of the petalite phase (Fig. 9a). In the surrounding glassy matrix there is no evidence of crystalline material of particle size greater than 5 nm, but within the dendrites there is a uniform distribution of dark particles which may well be a zirconia-rich phase that has become trapped during dendrite growth and that produces the weak, diffuse lines in the X-ray powder pattern. The poor nucleation efficiency of petalite, with a mean spacing of perhaps 1.5 to 2.0 μm between nucleating centres (Fig. 9b) suggests that it is not associated with the previous growth of a dendritic zirconia-rich phase in the same manner that pseudo-brookite precedes the growth of β-quartz in G362 ($11.5t$).

At 1000° C, the appearance of an alumina-rich spinel in G339 ($4t/7.5z$) before the exsolution of the silica-poor β-quartz commences suggests that the composition of the petalite phase is correspondingly both silica- and slightly magnesia-rich compared with the molar ratio $MgO:Al_2O_3:2.5SiO_2$. The early formation of spinel suggests that excess MgO and Al_2O_3 are indeed metastably

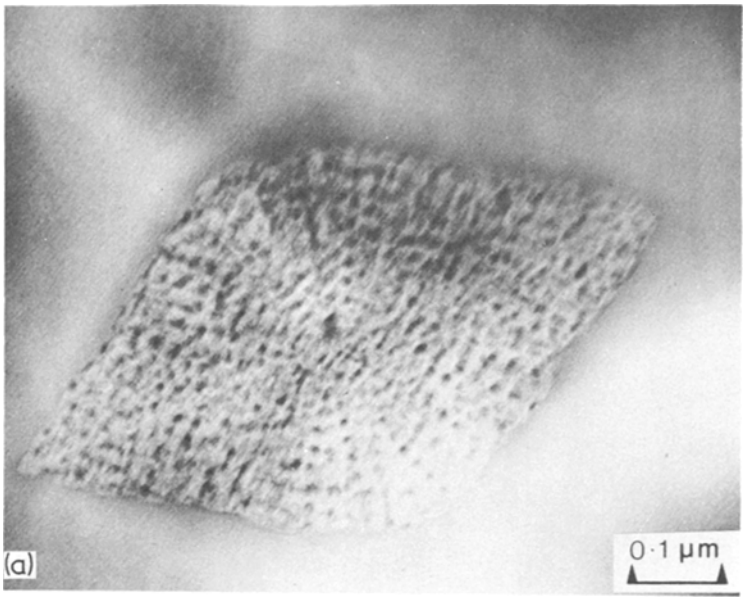

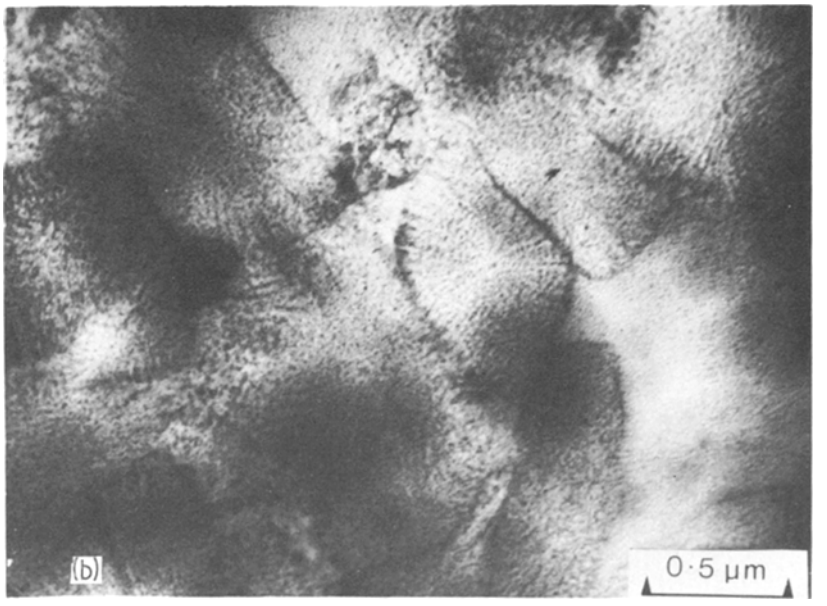

Figure 9 Magnesian petalite dendrites produced in G339 (4*t*/7.5*z*) (a) after heat treatment to 880° C only, (b) after heat treatment to 1000° C. Such dendrites are spaced about 1.5 to 2 μm apart.

associated with the $TiO_2 \cdot ZrO_2$ phase upon initial crystallization but are soon exsolved to a metastable spinel solid solution (Fig. 7*c*).

In the compositions in which petalite was found in this work, it was decreasing in concentration at 1050° C at the heating rate used, and had disappeared by 1100° C. It appears that in G339 (4*t*/7.5*z*) at least, it decomposes partly to cristobalite and cordierite, but mainly to β-quartz solid solution. Since the decomposition takes place at the same time as the start of the exsolution of β-quartz, it is not possible to determine whether spinel is also a decomposition product.

4.3. Exsolution of magnesia and alumina from β-quartz solid solution

The β-quartz solid solution in G362 (11.5*t*) originally contained less MgO and Al_2O_3 than that in compositions containing ZrO_2 in substitution for TiO_2. At temperatures above 1080° C, the slower rate of exsolution from the β-quartz in G362 causes it to have a relatively high content of MgO and Al_2O_3. As will be seen, this has important consequences at a later stage. No satisfactory explanation for the differences in rate exist at present, though it is interesting to note the equally mystifying differences in rate of exsolution for the

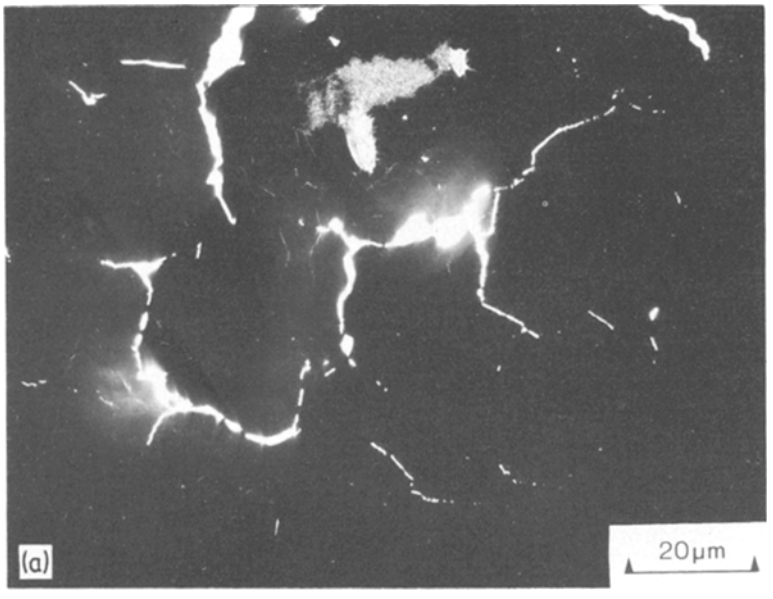

Figure 10 Cracks generated in G313 (1.9t/7.5z) after heating the glass to 1280° C and holding for 1 h, (a) electron shadowgraph of a section about 1 μm thick and (b) scanning electron micrograph of a fracture surface.

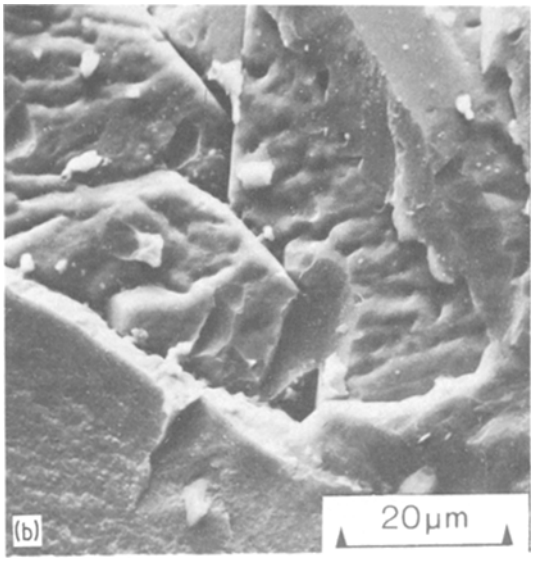

near surface and interior regions of both TiO_2- and ZrO_2-containing materials [3, 8, 18], and the absence of exsolution in compostions comprising MgO, Al_2O_3 and SiO_2 only.

4.4. Formation of cristobalite and cordierite

Examination of Figs. 6 and 7 shows that cristobalite develops to the greatest degree in those compositions in which the exsolution of magnesia and alumina proceeds to the greatest extent. When the β-quartz solid solution approaches pure SiO_2 in composition it becomes unstable, and at about 1220° C is converted to cristobalite. This occurs in compositions G339 (4t/7.5z) and G313 (1.9t/9.6z). For G362 (11.5t) not only is the exsolution slower, as discussed above, but it is also interrupted by the conversion to cordierite, and cristobalite does not form. For G354 (6.5t/5z) the exsolution was not significantly slower than for the compositions richer in ZrO_2 but the early formation of cordierite competes with that of cristobalite which is therefore produced in relatively small amounts.

However, with a more rapid heating schedule than the 5° C min^{-1} normally used, for example at 100° C min^{-1} used in unpublished studies, in both G362 (11.5t) and more especially G354 (6.5t/5z), high levels of cristobalite are found. Presumably this results from the influence heating rate has on the relative rates of exsolution from β-quartz, and back-reaction of β-quartz solid solution with the exsolved phases to form cordierite. If this is the case, it implies that cordierite formation is the more complex process of the two, requiring longer times at lower temperatures.

The role of the nucleant also has to be included in the discussion. Whereas in compositions G362 (11.5t) and G354 (6.5t/5z) there is sufficient TiO_2 to cause pseudo-brookite to be an initial phase, in G339 (4t/7.5z) and in G313 (1.9t/9.6z) pseudo-brookite is not present. This phase is not stable in the presence of β-quartz solid solution, whereas $TiO_2 \cdot ZrO_2$ and ZrO_2 are, and it may play a supplementary role in the overall conversion process when it decomposes to form rutile and spinel.

The practical consequences of the formation of cristobalite in glass–ceramics of this type are twofold. Firstly, if products containing large amounts

of cristobalite are cooled from within the range 1200 to 1250° C to room temperature, they crack spontaneously during the final stages of cooling. This appears to result from strain generated by the marked volume contraction of cristobalite on conversion from the β-phase to the α-phase at about 250° C. Secondly, if cristobalite is removed by heat treating for a sufficient duration at 1280° C (at least 1 h) to complete the conversion to cordierite, compositions G339 ($4t/7.5z$), G371 ($6.5t/6.5z$) and G313 ($1.9t/9.6z$) are found to suffer from gross cracking as well as being weak and friable. Microstructural examination shows them to be full of voids and cracks (Fig. 10). These cracks probably develop due to the sudden increase in volume that occurs when the silica rich β-quartz (cold density about 2.55 $Mg\,m^{-3}$) converts to β-cristobalite of rather lower density (about 2.16 $Mg\,m^{-3}$). In terms of the dilatometric length changes of samples on heating through the transformation range (Fig. 8), G362 ($11.5t$) and G354 ($6.5t/5z$) were found to convert fairly smoothly to cordierite commencing in the range 1150 to 1170° C. On the other hand G339 ($4t/7.5z$) and G313 ($1.9t/9.6z$) exhibited rather larger changes in length associated with the greater extent of exsolution and the onset of conversion to cristobalite in the range 1180 to 1200° C. Initial rapid jumps in lengths were found, followed by a levelling off and then a steady increase up to 1280° C. The initial jump correlates with the formation of large amounts of cristobalite as detected by its X-ray pattern, with the kink in thermal expansion behaviour of samples quenched during heat treatment, and also with a sharp exothermic feature in the DTA traces. In localized regions where conversion to cristobalite occurs, inhomogeneous volume changes lead to high local strains and result in crack production when plastic flow is insufficient to allow stress relief. Furthermore, if a block of material is not held within a narrow band of temperature, sudden increases in volume of one part of the block which is hotter than the remainder can impose long range thermal stresses which lead to gross cracking. Temperature, and hence conversion uniformity is therefore essential for the successful production of all cordierite glass–ceramics with little or no residual glass phase, and this poses a limit on block thickness because of the problems of removing exothermic heat fast enough to avoid rapid rises of temperature.

5. Summary and conclusions

(1) The relatively poor nucleation efficiency of TiO_2 in glasses of composition of that of cordierite ($MgO \cdot Al_2O_3 \cdot 2.5SiO_2$) is not improved by substitution of ZrO_2 for TiO_2 on a weight basis.

(2) Magnesian petalite is a major metastable phase during the initial crystallization in compositions in which both TiO_2 and ZrO_2 are present, with the greatest observed amount produced at a molar ratio $TiO_2:ZrO_2$ of about 1:1. Its formation depends on the prior phase separation of the glass, and once present affects the sequence of production of other phases. It decomposes to a mixture of β-quartz solid solution, cristobalite and cordierite at about 1050° C during 5° C min^{-1} heat treatment.

(3) The deformation that may be sustained by an article during heat treatment is related to the difficulty of nucleation of crystalline phases, is least for compositions containing TiO_2 only, and decreases with increasing TiO_2 content. Microstructural and X-ray studies show that deformation is reduced if a dendritic pseudo-brookite phase is formed first.

(4) The exsolution of spinel, and later sapphirine, from the β-quartz solid solution occurs at a rate dependent on the amount and type of nucleating agent added. The crystallographic unit cell dimensions of the β-quartz change progressively as exsolution proceeds, and the trend conforms with the pattern found in previous work on unnucleated systems.

(5) The absence of pseudo-brookite as a nucleating phase in higher ZrO_2 compositions increases the temperature at which conversion to cordierite occurs with the result that the β-quartz solid solution exsolves further and converts to cristobalite. Cordierite forms only at temperatures above 1220° C, instead of around 1150° C when pseudo-brookite is present.

(6) The appearance of cristobalite in large quantities is deleterious to the formation of a strong cordierite product after full conversion to the stable phases. The sudden increase in volume associated with the transformation of β-quartz solid solution to cristobalite leads to the formation of cracks on a fine scale, and to gross cracking in sections more than a few mm thick due to the fact that temperature homogeneity is never achieved in a violent exothermic situation.

Appendix

Phase characterization

Because of the complex nature of the phase assemblages developing in the glass-ceramics and the common occurrence of solid solutions and ill-defined phases, those phases occurring in the products are listed below with a description of relevant characteristics.

ZrO_2

In materials heated to above 1000° C, ZrO_2 can be identified as the tetragonal form. At lower temperatures the diffraction pattern is very diffuse due to the small particle size, and a distinction between cubic and tetragonal forms cannot be made. This has been noted by Dusil and Cervinka [5] who pointed out the similar diffraction patterns of tetragonal zirconia and cubic ZrO–MgO solid solutions. Beall and Duke [19] suggest that alumina may metastably be present in solid solution, a possibility supported by the fact that at about 1900° C, ZrO_2 takes up to 7% Al_2O_3 into stable solid solution [20]. At temperatures above about 1200° C where the tetragonal or cubic phase of ZrO_2 is stable, TiO_2 enters ZrO_2 in solid solution up to 20 mol% [21]. Metastable solid solutions are thus likely at lower temperatures.

$TiO_2 \cdot ZrO_2$

This phase has a diffraction pattern similar to ZrO_2, but is in fact distinct, with a range of solid solution for TiO_2 [22]. However, in the early stages of development, diffraction patterns of materials with compositions including both TiO_2 and ZrO_2 cannot be unambiguously assigned to $TiO_2 \cdot ZrO_2$ or to ZrO_2, due presumably to the very fine particle size.

TiO_2

Rutile with a normal diffraction pattern is the only TiO_2 phase identified.

Pseudo-brookite solid solutions

In the $MgO–Al_2O_3–TiO_3$ system, pseudo-brookite has a range of existence along the composition limits Al_2TiO_5 to $MgTi_2O_5$. The phase is stable only above a temperature which varies from 1262° C to about 1000° C along this composition join [23]. The composition can be determined by X-ray diffraction with the aid of standards.

Spinel

The composition has a stoichiometry close to $MgAl_2O_4$ based on unit cell dimensions, except where mentioned in the text. An extensive range of solid solutions with Al_2O_3 and/or TiO_2 exists at high temperatures and also probably metastably at low temperatures. SiO_2 may also enter solid solution, and recent information confirms this [24].

Sapphirine

This phase has a composition approximating to $Mg_2Al_4SiO_{10}$ but natural and synthetic crystals are usually richer in alumina than this with 2Al replacing Mg + Si. In the glass–ceramics it forms as an exsolution product of β-quartz solid solution at a later stage than spinel, which it replaces. The exact composition of the sapphirine that developed in the present work is unknown but to simplify consideration of the crystal phase development, the composition $Mg_2Al_4SiO_{10}$ was assumed in the calculation of Fig. 7.

β- or high- quartz solid solution (sometimes undesirably named μ-cordierite)

The β-quartz SiO_2 structure can take $MgAl_2O_4$ into metastable solid solution over a wide range of composition and at least up to $MgO \cdot Al_2O_3 \cdot 2SiO_2$. The Al^{3+} ions normally occupy silicon sites and the Mg^{2+} ions interstitial sites. Only when there is a deficiency of other suitable ions will Al^{3+} ions occupy interstitial sites [25]. Schreyer and Schairer [13] found that the unit cell dimensions of $MgO \cdot Al_2O_3 \cdot nSiO_2$ solid solutions were linearly dependent on the weight proportion of SiO_2, but subsequent studies [14, 15] showed that ordered superstructures formed with prolonged heat treatment of the silica-poor compositions and caused some variation in the dimensions of the basic unit cell. Superstructure lines were not observed in the nucleated materials of the present study.

α-quartz

When the silica content of the β-quartz solid solution is greater than about 85% the structure converts to α-quartz on cooling. The transition as indicated by dilatometric studies becomes sharper and moves to higher temperatures as the silica content of the phase increases. However the transition temperature is not solely dependent on composition, it is also a function of grain size.

Magnesian petalite

Schreyer and Schairer [13] discovered that a phase with an X-ray diffraction pattern akin both to the natural mineral petalite, $Li_2O \cdot Al_2O_3 \cdot 8SiO_2$, and to synthetic lithium disilicate $Li_2O \cdot 2SiO_2$, which have similar structures [26], could develop in heat-treated $MgO-Al_2O_3-SiO_2$ glasses. The composition was thought to lie within the triangle bounded by the molar $MgO:Al_2O_3:SiO_2$ ratios of 1:0:2, 1:1:8, 1:1:3. However, it could not be grown from glasses on the edges or corners of this triangle. Subsequently, Holmquist [17] found that this phase, which was characterized in his products by two strong lines at about 3.74 and 3.66 Å, was developed in a glass of composition $MgO \cdot Al_2O_3 \cdot 3SiO_2$ + 10 wt% ZrO_2 by long periods of treatment at relatively low temperatures, and more strongly when the $MgO:Al_2O_3:SiO_2$ ratio was changed to 1:1:4.3. Dusil and Cervinka [5] obtained similar results in a glass of $MgO:Al_2O_3:SiO_2$ ratio of 1:0.4:2.8. In the present work, the composition assumed for the petalite-like phase is 1:1:3. Any significantly higher silica content would be inconsistent with the overall composition and that of the other phases present, and a lower silica content would be inconsistent with the fact that petalite is generated most easily in compositions richer rather than poorer in silica.

The X-ray '*d*-spacings' observed correlate well with those of Holmquist except that there is a general shift to lower values. The results (in Å units) listed below were obtained for G339 (4*t*/7.5*z*) heated to 1000° C.

7.10 mw, 3.72 vs, 3.62 s, 3.54 w, 2.63 wd, 2.54 w, 2.47 w, 2.360 w, 2.245 w, 2.041 mw, 1.920 mw, 1.715 w, 1.618 w.

s = strong, m = medium, w = weak, v = very, d = diffuse.

The line at 2.47 Å may have been shifted by a neighbouring spinel line.

Cristobalite

Cristobalite develops during heat treatment of ZrO_2-containing compositions at about 1200° C. It is assumed to be pure SiO_2 and its relative proportion can be estimated from the magnitude of the change in expansion coefficient consequent upon the α, β inversion at about 250° C. Cristobalite is metastable relative to β-quartz below about 1130° C. Thus, if it is formed at lower temperatures, it probably derived from another source. Tridymite is said to be the stable SiO_2 phase in this temperature region but it has not been observed in the present work.

Cordierite

The anhydrous form of cordierite stable below 1440° C is the low (orthorhombic) one. Between 1440° C and the incongruent melting point of 1455° C a high (hexagonal) form is the stable phase. Its composition is nominally $MgO \cdot Al_2O_3 \cdot 2.5SiO_2$ with a limited solid solution range in which $Mg^{2+} + Si^{4+}$ replaces $2Al^{3+}$. A metastable hexagonal form is found by X-ray diffraction in the glass-ceramics of this study, but it is possible that in fact the product really comprises microdomains of low cordierite assembled to give apparently hexagonal symmetry [27, 28].

Acknowledgements

The authors wish to express their appreciation for the help of D. J. Clinton and L. A. Lay in the course of this work.

References

1. S. D. STOOKEY, US Patent 2 920 971, 1960.
2. T. I. BARRY, L. A. LAY and R. MORRELL, *Proceedings of the Brit. Ceram. Soc.* **22** (1973) 27.
3. *Idem, Science of Ceramics* **8**, (1976) 331.
4. G. F. NEILSON, "Advances in Nucleation and Crystallization in Glasses", (American Ceramic Society, Columbus, 1971) p. 73.
5. J. DUSIL, L. CERVINKA, *Glass Technol.*, **17**, (1976) 106.
6. M. A. CONRAD, *J. Mater. Sci.* **7**, (1972) 527.
7. W. ZDANIEWSKI, *J. Amer. Ceram. Soc.*, **58** (1975) 163.
8. R. W. TUCKER and D. R. STEWART, Proceedings of the IXth International Congress on Glass 1971, edited by Institut du Verre (International Congress on Glass, Paris, 1971) p. 1119.
9. D. R. STEWART, "Advances in Nucleation and Crystallization in Glasses"' (American Ceramic Society, Columbus, 1971) p. 83.
10. H. SCHEIDLER and W. SACK, Proceedings of the IXth International Congress on Glass, 1971, edited by Institut du Verre (International Congress on Glass, Paris, 1971) p. 1064.
11. T. I. BARRY, L. A. LAY and R. MORRELL, *Proc. Brit. Ceram. Soc.*, **25** (1975) 67.
12. H. E. HAGY, US Patent 3 129 087, 1964.
13. W. SCHREYER and J. F. SCHAIRER, *Zeits. Krist.* **116** (1961) 60.
14. H. SCHULZ, G. M. MUCHOW, W. HOFFMAN and G. BAYER, *ibid* **133** (1971) 91.
15. H. SCHULZ, W. HOFFMAN and G.M. MUCHOW, *ibid* **134** (1971) 1.

16. W. SCHREYER and J. F. SCHAIRER, *Amer. Min.* **47** (1962) 90.
17. S. B. HOLMQUIST, *Zeits, Krist.* **118** (1963) 477.
18. Corning Glass Works, UK Patent 940 403, 1963.
19. G. H. BEALL and D. A. DUKE, *J. Mater. Sci.* **4** (1969) 340.
20. A. M. ALPER, *Science of Ceramics* **3** (1967) 335.
21. A. ONO, *Miner. J.*, **6** (1972) 433.
22. L. W. CONGHANOUR, R. S. ROTH and V. A. DE PROSSE, *J. Res. Natl. Bureau. Stds.* **52** (1974) 37.
23. P. BODEN and F. P. GLASSER, *Trans. Brit. Ceram. Soc.* **72** (1973) 215.
24. R. SMART and F. P. GLASSER, private communication.
25. G. H. BEALL, B. R. KARSTETTER and H. L. RITTLER, *J. Amer. Ceram. Soc.* **59** (1967) 181.
26. F. LIEBAU, *Acta. Cryst.* **14** (1961) 399.
27. K. LANGER and W. SCHREYER, *Am. Miner.* **54** (1969) 1442.
28. S. P. YURKOVITCH, PhD Thesis, Univeristy of Michigan, Ann Arbor, Michigan, USA, 1972.

Received 10 May and accepted 17 June 1977.